

## Inner-valence states of CO<sup>+</sup> between 22 eV and 46 eV studied by high resolution photoelectron spectroscopy and *ab initio* CI calculations

P Baltzer<sup>†</sup>, M Lundqvist<sup>†</sup>, B Wannberg<sup>†</sup>, L Karlsson<sup>†</sup>, M Larsson<sup>‡</sup>,  
M A Hayes<sup>§</sup>, J B West<sup>§</sup>, M R F Siggel<sup>§</sup>, A C Parr<sup>||</sup> and J L Dehmer<sup>¶</sup>

<sup>†</sup> Uppsala University, Department of Physics, Box 530, S-751 21 Uppsala, Sweden

<sup>‡</sup> Royal Institute of Technology, Physics 1, 100 44 Stockholm, Sweden

<sup>§</sup> Daresbury Laboratory, Warrington WA4 4AD, UK

<sup>||</sup> National Institute of Standards and Technology, Gaithersburg, MD 20899, USA

<sup>¶</sup> Argonne National Laboratory, Argonne, IL 60439, USA

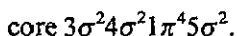
Received 13 June 1994, in final form 11 August 1994

**Abstract.** Photoionization of the CO molecule and inner-valence states of CO<sup>+</sup> between 22 and 45 eV have been studied by means of photoelectron spectroscopy using both synchrotron radiation and He I radiation. Vibrational structure has been resolved in many bands up to 45 eV. CASSCF (complete active space self-consistent field) and MRCI (multireference configuration interaction) calculations of potential curves in the 22–30 eV range have been performed and these have been used to predict vibrational levels and Franck–Condon factors. In this energy range three valence states, D<sup>2</sup>Π, 3<sup>2</sup>Σ<sup>+</sup> and 3<sup>2</sup>Π have been identified, and spectroscopic constants have been determined for the first two of these. Above 30 eV, all valence states have been found to be repulsive. In addition to the broad bands expected for these states, several progressions of narrow lines are observed most probably reflecting transitions to Rydberg states.

### 1. Introduction

Inner valence UV photoelectron spectra often exhibit complex bands due to many-electron processes in addition to the main bands expected from an independent electron picture. A good description of these spectra generally requires consideration of configuration mixing in the final state as well as in the initial state (Cederbaum and Domcke 1977, Martin and Shirley 1976) as has been demonstrated most recently for the photoelectron spectrum of N<sub>2</sub> by Baltzer *et al* (1992a). For small molecules, these inner-valence photoelectron bands contain vibrational structure and this provides an excellent opportunity to obtain experimental information about the potential energy curves.

The three lowest electronic states of CO<sup>+</sup> can be described essentially in terms of the single-hole states arising as a result of ionization from the 5σ, 1π and 4σ orbitals. This assumes writing the ground state electron configuration of CO as



These outer-valence electronic states are readily studied by He I photoelectron spectroscopy; see, for example, Turner *et al* (1970), Wannberg *et al* (1988) and Edvardsson *et*

*al* (1994). At higher energies, above approximately 20 eV, the number of states increases quickly due to significant many-electron effects and this leads to a breakdown of the independent-particle molecular orbital approximation. The  $3\sigma^{-1}$  hole state is split into a manifold of  ${}^2\Sigma^+$  states (Okuda and Jonathan 1974, Schirmer *et al* 1977, Bagus and Viinikka 1977, Cederbaum *et al* 1980, Langhoff *et al* 1981, Ågren and Arneberg 1983) which may be reached in the photoionization process. State mixing involving the outer-valence, single-hole states is also important to explain some of the weaker features observed in the inner-valence region.

Potts and Williams (1974), Åsbrink *et al* (1974), Codling and Potts (1974), Carlsson Göthe (1990) and Carlsson Göthe *et al* (1991) have reported experimental inner-valence studies previously using He II radiation. Synchrotron radiation studies have been made by Krummacher *et al* (1980, 1983) and Liu *et al* (1993) and xps (x-ray photoelectron spectroscopy) measurements with Y M $\zeta$  (132 eV) by Banna and Shirley (1976) and Nyholm *et al* (1977) and with Al K $\alpha$  (1487 eV) by Gelius *et al* (1973) and Svensson *et al* (1991). In the most recent studies using UV (Carlsson Göthe) and x-ray (Svensson *et al*) excitation, assignments of the inner valence bands have been suggested from comparisons also with resonance Auger spectra from Eberhardt *et al* (1987) and the potential curve of the well known  $3^2\Sigma^+$  state has been derived. In the present investigation, we have used both He II radiation and synchrotron radiation at the photon energies 36, 40, 44 and 46.4 eV to obtain improved experimental data, facilitating the analysis of this complicated spectrum, and we present a more general discussion of potential curves. The He II excited spectra are better resolved and have much better signal-to-background ratios than obtained previously. The synchrotron radiation photoelectron spectra were recorded at a photoelectron linewidth of about 30 meV and exhibit vibrational structure even in the range above 30 eV, as was reported also by Liu *et al* (1993) whose experimental linewidth was  $\sim$ 100 meV. Many lines and progressions have been accurately determined by comparison to the lines produced by He II $\beta$  radiation and which appear at much lower energies in the He II excited spectrum.

Potential curves relevant to the present results for states up to about 25 eV have recently been published in two studies (Lavendy *et al* 1993, Honjou and Yarkony 1985) using configuration interaction (CI) methods. However, for the interpretation of the photoelectron spectrum some details in the potential curves need to be further clarified, and potential curves need to be studied at even higher energies than considered in these reports. We have therefore carried out new CI calculations of the potential curves.

The notations of the electronic states in the inner valence region vary substantially between different authors. For simplicity therefore we number all states of the same symmetry consecutively from lower to higher energy. The same numbering was used also in the recent theoretical work by Honjou and Yarkony. This means that the state often referred to as C  ${}^2\Sigma^+$  is labelled  $3^2\Sigma^+$  in the present study. For the outer valence states and also the inner valence D  ${}^2\Pi$  state the old notations are consistent and are therefore retained.

## 2. Experimental details

The He II excited spectra were recorded on a high resolution photoelectron spectrometer that has been described earlier in some detail by Baltzer *et al* (1993). It is equipped with a microwave powered electron cyclotron resonance UV source that provides a high He II intensity and very narrow resonance radiation (Baltzer and Karlsson 1989).

Recent improvements have resulted in a substantial enhancement of the signal-to-background ratio for the spectrometer and a value of  $10^5$  has been measured for the Ar 3p lines. This is particularly important for inner valence studies since the photoelectron lines are very weak.

The spectra were calibrated using the recoil corrected binding energy 24.589 eV for He 1s. All spectra are shown exactly as they were obtained from the spectrometer without background subtraction. The energies, widths and relative intensities of the lines have been determined by a procedure where Gaussian lines have been fitted to the experimental data. The centre of the fitted line has been used to represent the position of each line. The positions of well defined lines are accurate to better than 1 meV.

The Synchrotron Radiation Source at Daresbury laboratory was used to collect spectra at wavelengths in addition to those obtainable from the helium discharge, and for studies of angular distributions of the photoelectrons. A 5 m normal incidence monochromator provided monochromatic radiation, and when the resolution of this was combined with the photoelectron spectrometer resolution, line widths  $\sim 30$  meV were obtained. The photoelectron spectra were recorded on a spectrometer system that has been used extensively for studies of photoionization cross sections and angular distributions and has been described in detail by Parr *et al* (1984). In summary, it comprises two 100 mm mean radius hemispherical electron spectrometers, one of which is fixed to accept electrons ejected along the major polarization component of the incoming photon beam and the other is rotatable about the light beam axis. Both spectrometers are fitted with area detectors at their exit planes, and an analyser to measure the polarization of the incoming light is included in the system. Measurements were made both perpendicular and parallel to the  $E$ -vector of the incident radiation simultaneously, and after relative calibration of the spectrometers the system provides both partial cross sections and photoelectron angular distributions, using the expression for the differential photoionization cross section.

Inelastic scattering of photoelectrons gives rise to additional lines in the spectra. To verify that the states invoked in the interpretation are strongly excited by electrons we have recorded an electron impact spectrum of CO using an apparatus designed in Uppsala (Baltzer 1994). It uses a zero energy detection system similar to that described by Schlag *et al* (1993).

### 3. Computational details

The potential curves used in this work were calculated by means of a two-step procedure. In the first step, multiconfiguration self-consistent-field (SCF) calculations were performed using the complete active space SCF (CASSCF) approach (Siegbahn *et al* 1981). The nine valence electrons were distributed in all possible ways into the  $3\sigma$ ,  $4\sigma$ ,  $5\sigma$ ,  $6\sigma$ ,  $1\pi$  and  $2\pi$  orbitals. In other words, both the 2s and 2p orbitals and their electrons are active. This gave 616 configuration state functions (CSFs) for electronic states of  $^2\Sigma^+$  symmetry and 588 CSFs for states of  $^2\Pi$  symmetry. Since many electronic states in each symmetry were needed, the molecular wavefunctions were obtained by a state-averaged procedure. This means that a single set of CASSCF orbitals was obtained for states of  $^2\Sigma^+$  and  $^2\Pi$  symmetry, respectively. The calculations were performed in  $C_{2v}$  symmetry, which means that some caution was needed to separate  $^2\Sigma^+$  from  $^2\Delta$  states appearing in the same  $C_{2v}$  symmetry. The basis sets for carbon and oxygen were the

[6s4p] Lie and Clementi (1974) contractions of van Duijneveldt (1971) (10s6p) primitive sets. These were augmented with d functions from Lie and Clementi and f functions with exponents 0.8 and 1.313 for carbon and oxygen, respectively. This [6s4p2d1f] basis set was considered sufficient for the present purpose.

In the second step, multireference CI (MRCI) calculations in a contracted scheme (Siegbahn 1983) was used based on the CASSCF zero-order reference functions. No threshold procedure was adopted and hence all CSFs from the CAS were used as reference states. Both the 2s and 2p electrons were correlated, while the two 1s-like core orbitals were constrained to be doubly occupied.

## 4. Results

### 4.1. The overall spectrum

Figure 1 shows the overall He II excited photoelectron spectrum over the 21–29 eV region where no overlap with the highly intense He I excited spectrum occurs. Five bands can be seen in this region, in agreement with the observations from the spectrum obtained with monochromatized He II $\alpha$  radiation by Carlsson Göthe (1990). Vibrational structure is observed in four of these, while the fifth band centred at 27.4 eV is structureless. However, as will be shown below, two of these, the bands at 25 eV and the main part of the band between 27.6 and 29 eV, do not reflect electronic states in these regions but are due to inelastic scattering of photoelectrons and excitations with He II $\beta$  radiation. Nevertheless, in both regions a rather high and essentially constant intensity is observed. This is not solely due to the spectrometer background, which is responsible for the intensity seen on the far right side of the spectrum, but must in part be associated with photoionization processes in CO. Presumably, it reflects transitions involving repulsive parts of the potential curves in this energy range. The He I s line is observed at 24.589 eV.

Figure 2 shows the full spectrum obtained with synchrotron radiation at 46.4 eV. This spectrum covers, in addition to the region recorded by the He II excitation, the main part of the 3 $\sigma^{-1}$  region and also the first 3 eV of the double ionization continuum which starts at 41.7 eV (Correia *et al* 1985). Due to a low signal-to-background ratio, there is substantial scattering in the data but the main features are well defined and agree with earlier spectra of this region recorded at lower resolution using synchrotron radiation and XPS. Numerous narrow lines can be seen, but only those lines which appear in all spectra and have consistent  $\beta$ -values will be discussed.

### 4.2. The 22–25 eV range

In figure 1, transitions to the D<sup>2</sup> $\Pi$  and 3<sup>2</sup> $\Sigma^+$  cationic states of the He II excited photoelectron spectrum can be seen in the 22–25 eV range. The B<sup>2</sup> $\Sigma^+$  state appears in the first part of the figure due to the 320 Å component in the He I radiation. The  $v=0, 1$  and 2 components of this vibrational progression can be seen clearly at line positions that agree with the earlier experiments by Potts and Williams (1974) and Åsbrink *et al* (1974).

The first lines associated with the D<sup>2</sup> $\Pi$  state, which has the leading configurations 5 $\sigma^{-2}2\pi^1$  and 4 $\sigma^{-1}5\sigma^{-1}2\pi^1$ , appear in the 22.2–22.4 eV range. This is shown in some detail in figure 3. Due to the overlap with the lines corresponding to the B state, the

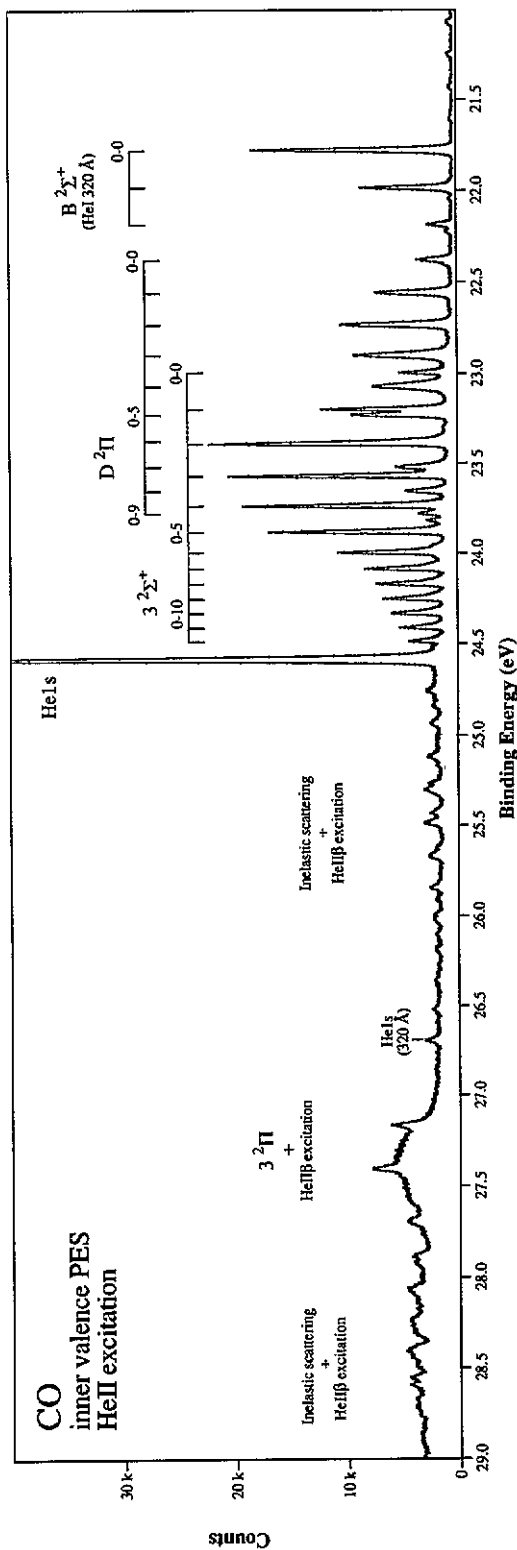


Figure 1. The inner valence photoelectron spectrum of CO obtained with He IIα radiation at 40.8 eV.

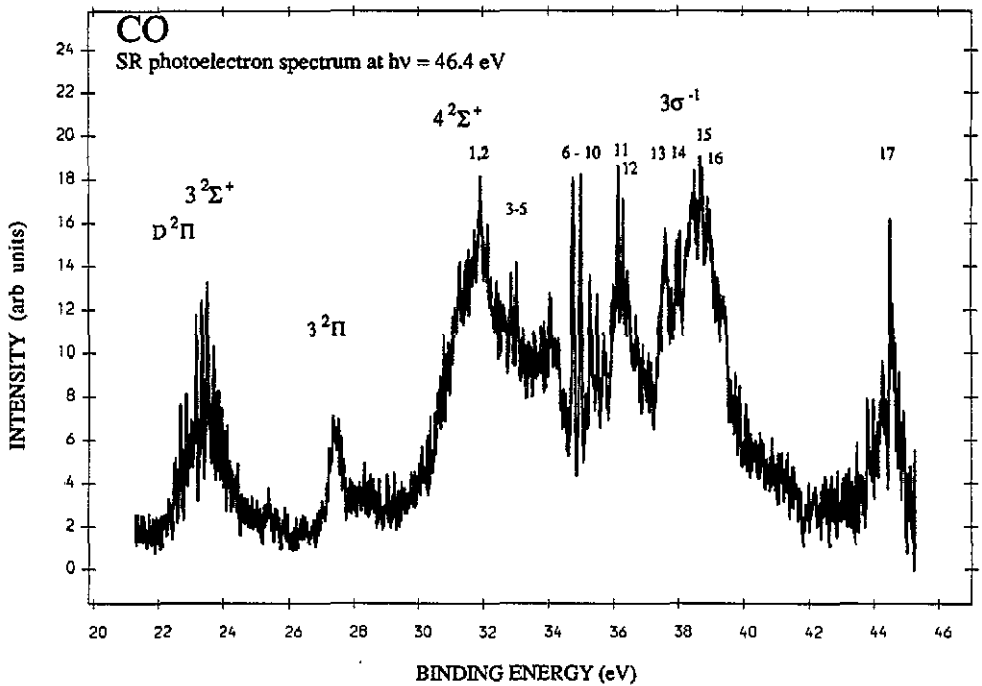


Figure 2. The inner valence photoelectron spectrum of CO obtained with synchrotron radiation at 46.4 eV.

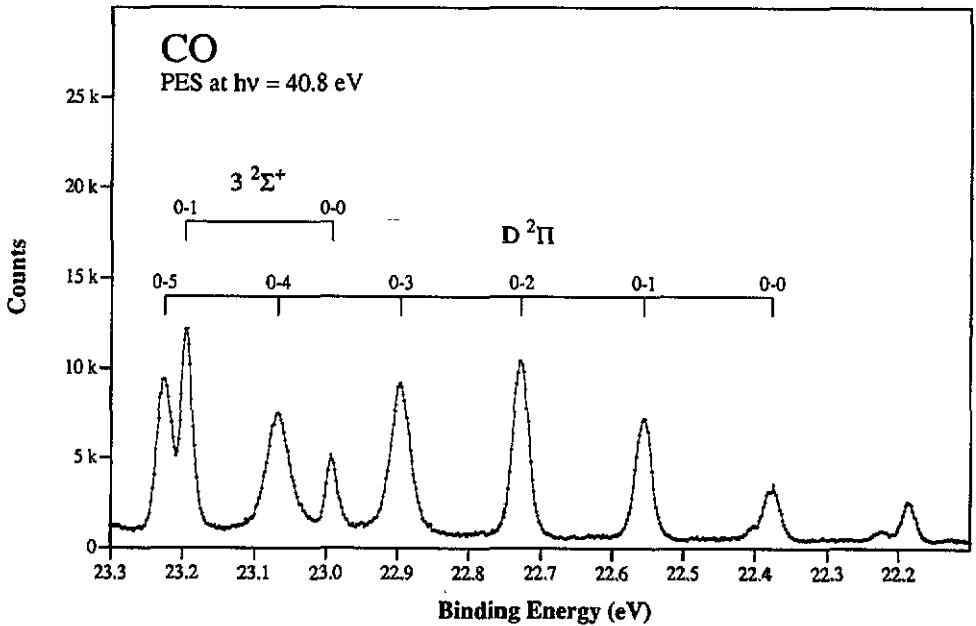


Figure 3. Detail of the He II excited photoelectron spectrum of CO in the 22.3–23.3 eV range showing transitions to the  $D^2\Pi$  and  $3^2\Sigma^+$  cationic states. A weak line observed at 22.403 eV is due to inelastic scattering of photoelectrons from the  $5\sigma$  orbital.

0-0 transition has not been clearly identified in earlier studies. The present results strongly favour the line at 22.378 eV, which fits very well into the vibrational progression and has a relative intensity close to the calculated Franck-Condon factor. The line at 22.187 eV fits reasonably well with the vibrational progression. However, comparison with the He  $\pi\alpha$  excited spectrum of the B  $^2\Sigma^+$  state shows that at least the dominant part of its intensity should be assigned to the  $\nu=2$  line of this state, excited by 320 Å He I radiation. Then, the remaining part of its intensity is much too low in comparison with the calculations. The second possible candidate observed at 22.224 eV would give an unexpectedly small vibrational spacing, 156 meV compared to 179 meV for the next

**Table 1.** Binding energies and relative intensities obtained for transitions to the D  $^2\Pi$  state of CO<sup>+</sup>. The experimental data were obtained from the He  $\pi$  excited spectrum and for the calculated binding energies the reference level was A  $^2\Pi(\nu=0)$ .

Vibr. quant. no	Binding energy (eV)		Vibrational spacing (meV)		Line width FWHM (meV)	Relative intensity	
	Expt	Calc.	Expt	Calc.	Expt	Expt	Calc.
0	22.378	22.451			25.9	0.28	0.218
1	22.557	22.622	179	171	25.9	0.65	0.597
2	22.729	22.787	172	165	25.9	0.95	0.880
3	22.897	22.950	168	163	31.0	1.00	1.000
4	23.069	23.114	172	164	36.7	0.95	0.914
5	23.227	23.271	158	157	25.9	0.84	0.712
6	23.372	23.418	145	147	25.9	0.65	0.515
7	23.521	23.555	149	137	30.6	0.54	0.357
8	23.655	23.681	134	126	25.9	0.38	0.237
9	23.779	23.795	124	114	28.3	0.28	0.152
10		23.888		93			0.084

two lines, and its intensity is also much too low compared to the calculations. Table 1 summarizes the energies, linewidths and relative intensities of this progression obtained in the present study. It may be noted that the experimental intensity given in table 1 for the 0-0 line is slightly too high due to an unresolved overlap with the B  $^2\Sigma^+$  ( $\nu=3$ ) line. It is noteworthy also, that the lines of the D  $^2\Pi$  state are generally much broader than those of other electronic states in the same region. This is expected, considering the spin-orbit splitting. A curve fitting using the C state lineshape as a model gives a splitting of 12 meV which is close to the predicted value  $\sim 10$  meV from the recent calculation by Lavendy *et al* (1993).

The vibrational energies decrease gradually and from the experimental data the following spectroscopic constants can be derived for the D  $^2\Pi$  state:  $T_e = 67\,805 \pm 15$  cm<sup>-1</sup>,  $\omega_e = 1530 \pm 15$  cm<sup>-1</sup> and  $\omega_e x_e = 26.7 \pm 9$  cm<sup>-1</sup>.

A substantial broadening is observed of the  $\nu=3$  and 4 lines (cf table 1) and the vibrational spacings are also somewhat irregular. This could be caused by a crossing with the 3 $^2\Pi$  potential curve that is predicted in this energy region, as will be further discussed below.

The 3 $^2\Sigma^+$  state (leading configuration  $5\sigma^{-1}1\pi^12\pi^1$ ) is much better resolved than in the previous study by Carlsson Göthe *et al* (1991) and the 0-0 transition is readily observed at 22.993 eV. The 0-1 vibrational spacing is 203 meV and the following spacings decrease by about 10 meV per step up to the  $\nu=4$  level, corresponding to a significant anharmonicity in the potential curve. From these energies, summarized in table 2,

**Table 2.** Binding energies and relative intensities obtained for transitions to the  $3^2\Sigma^+$  state of  $\text{CO}^+$ . The experimental data were obtained from the He II excited spectrum and for the calculated binding energies the reference level was  $X^2\Sigma^+(v=0)$ .

Vibr. quant. no	Binding energy (eV)		Vibrational spacing (meV)		Line width FWHM (meV)	Relative intensity	
	Expt	Calc.	Expt	Calc.	Expt	Expt	Calc.
0	22.993	22.989			19.7	0.24	0.171
1	23.196	23.190	203	201	18.8	0.59	0.507
2	23.388	23.382	192	192	18.8	0.97	0.838
3	23.570	23.561	182	179	18.8	1.00	1.000
4	23.737	23.722	167	161	18.8	0.93	0.952
5	23.882	23.856	145	134	18.8	0.82	0.767
6	23.998	23.996	116	140	18.8	0.51	0.630
7	24.089	24.064	91	68	18.8	0.38	0.528
8	24.171	24.155	82	91	18.8	0.33	0.458
9	24.253	24.242	82	87	19.7	0.32	0.408
10	24.333	24.330	80	88	20.7	0.29	0.363
11	24.412	24.417	79	87	20.7	0.24	0.317
12	24.489	24.502	77	85	20.7	0.20	0.254

the following spectroscopic constants have been derived for the region up to  $v=4$ :  $T_e = 72\,676 \pm 40 \text{ cm}^{-1}$ ,  $\omega_e = 1720 \pm 30 \text{ cm}^{-1}$  and  $\omega_e x_e = 49 \pm 30 \text{ cm}^{-1}$ .

From  $v=5$  to  $v=8$  the vibrational spacings are much reduced, whereafter the spacings are about 80 meV. This behaviour of the vibrational structure was reported earlier by Potts and Williams and Carlsson Göthe *et al* and explained in terms of a broadening of the potential curve due to a strongly avoided curve crossing, which agrees with the theoretical results of the present study and those of Honjou and Yarkony. Unfortunately, the end of the progression is not observed clearly in the He II excited spectrum due to the presence of the He I s line at 24.589 eV. However, expanding the SR spectrum in this region shows that the last well defined line is clearly the  $v=12$  component. At higher energies an enhancement of the 'background' level can be seen, particularly in the He II excited spectrum, which suggests that in this range the transitions involve the repulsive part of the  $3^2\Sigma^+$  state potential curve. It may be noted that the very weak line at 24.520 eV is not associated with the  $3^2\Sigma^+$  state but is a satellite due to the He II radiation.

The lines belonging to the  $3^2\Sigma^+$  state are asymmetric with a tail on the low binding energy side that is very pronounced for the higher vibrational components (cf figure 4). This is due to the inherent rotational fine structure and shows that the average internuclear distance is larger in the  $3^2\Sigma^+$  state than in the neutral ground state, and increases considerably with the vibrational quantum number.

From the spectra taken with synchrotron radiation the asymmetry parameter  $\beta$  has been determined for the individual vibrational lines. The data are summarized in table 3 along with the relative intensities obtained in the spectra recorded at  $0^\circ$ , i.e. in the same direction as the major polarization component of the incident radiation. Two qualitative observations can be made: First, the relative intensity tends to decrease with increasing photon energy, which follows the behaviour generally observed in this energy region. Second, the  $\beta$ -values differ markedly between the two progressions which confirms the interpretation in terms of two separate electronic states.

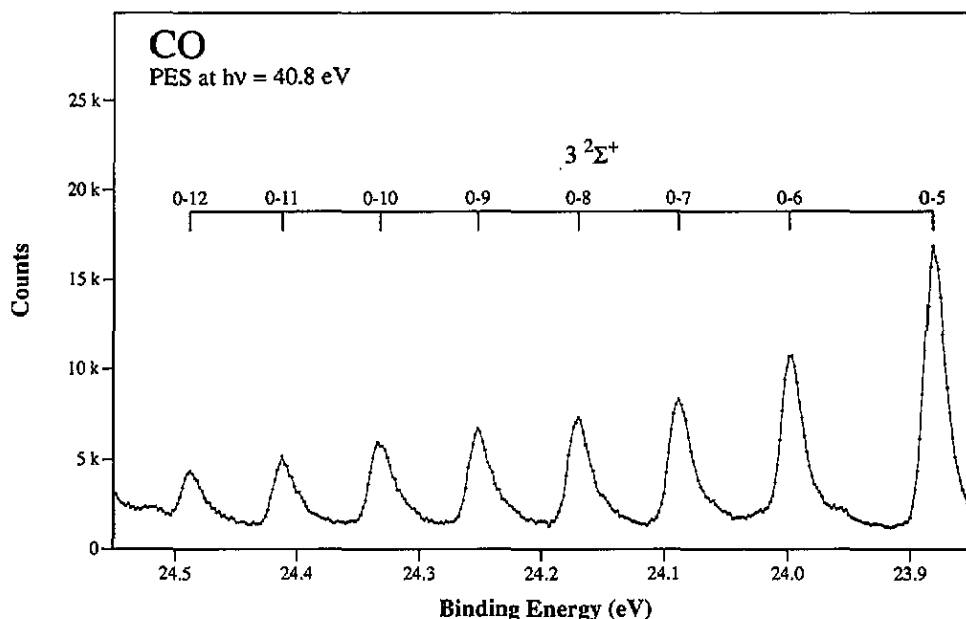


Figure 4. Detail of the He II excited photoelectron spectrum of CO in the 23.85–24.55 eV range showing the uppermost part of the  $3^2\Sigma^+$  vibrational progression.

Table 3. Summary of relative intensities and  $\beta$  values obtained from synchrotron radiation photoelectron spectra at 36 eV, 40 eV and 44 eV photon energies for the bands associated with the  $D^2\Pi$  state and  $3^2\Sigma^+$  state of CO<sup>+</sup>. Errors shown represent one standard deviation from the mean value.

State and vibr. quant. no	Binding energy (eV)	Intensity			$\beta$		
		36 eV	40 eV	44 eV	36 eV ( $\pm 0.1$ )	40 eV ( $\pm 0.1$ )	44 eV ( $\pm 0.1$ )
$D^2\Pi(0)$	22.378	0.20	0.14	0.15	0.3	0.4	0.0
$D^2\Pi(1)$	22.557	0.51	0.34	0.34	0.4	0.3	0.2
$D^2\Pi(2)$	22.729	0.68	0.49	0.42	0.3	0.2	0.3
$D^2\Pi(3)$	22.897	0.75	0.52	0.49	0.1	0.4	0.0
$D^2\Pi(4)$	23.069	0.59	0.47	0.39	0.4	0.3	0.1
$3^2\Sigma^+(0)$	22.993	0.23	0.24	0.20	1.0	1.3	1.0
$3^2\Sigma^+(1)$	23.196	0.80	0.62	0.53	0.6	0.8	0.8
$3^2\Sigma^+(2)$	23.388	0.79	0.72	0.65	0.7	0.9	0.8
$3^2\Sigma^+(3)$	23.570	0.64	0.63	0.47	0.7	1.3	1.5
$3^2\Sigma^+(4)$	23.737	0.55	0.47	0.37	1.1	1.5	1.7
$3^2\Sigma^+(5)$	23.882	0.40	0.38	0.38	1.3	1.4	1.4
$3^2\Sigma^+(6)$	23.998	0.28	0.32	0.25	1.1	1.4	1.5
$3^2\Sigma^+(7)$	24.089	0.21	0.23	0.18	1.3	1.4	1.6

#### 4.3. The 25–27 eV range

Weak vibrational structure is seen in the 25–26 eV range (cf figure 1). A corresponding structure was observed earlier in the monochromatized He II excited spectrum taken by Carlsson Göthe (1990) and also by Åsbrink *et al* where it was referred to as the sixth progression. The present calculations give no support for an assignment in terms

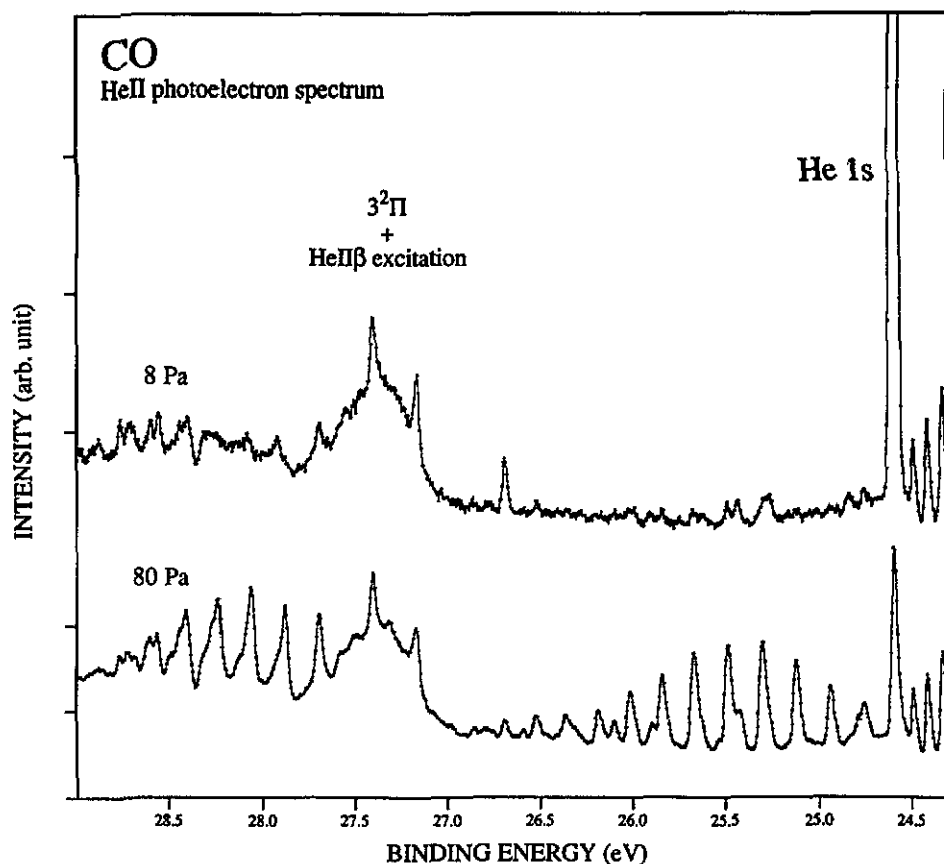


Figure 5. He II excited inner valence photoelectron spectra of CO between 24.7 eV and 29 eV recorded at two different pressures, 8 and 80 Pa, to show the pressure dependence of many lines in this energy region. The pressures are measured in the inlet line to the gas cell, and the actual sample pressure is about ten times lower.

of a many-electron state of  $^2\Sigma^+$  or  $^2\Pi$  symmetry, which are the only symmetries that would acquire a considerable photoelectron intensity. Furthermore, the intensity of these lines is pressure dependent. In figure 5 we show two spectra recorded at very different pressures, and in the low pressure spectrum, most of the lines have disappeared almost completely. This gives very clear evidence that the lines are due to inelastic scattering of photoelectrons. Energetically, the lines fit exactly with excitations to the a  $^3\Pi$  and A  $^1\Pi$  states of neutral CO caused by photoelectrons ionized from the  $1\pi$  orbital by the He II line. Both these states are strongly excited as shown by the electron impact spectrum of figure 6. Moreover, pressure-dependent lines are observed in the 22.4 eV and 27.5 eV regions, which would be expected for scattering of photoelectrons from the  $5\sigma$  and  $4\sigma$  orbitals. However, several lines remain even at very low pressures. They can be associated with ionization by the He II $\beta$  component and thus correspond to states at energies 7.558 eV higher than their apparent position, as will be discussed below. To the extent that they can be unambiguously identified with features in the synchrotron radiation photoelectron spectrum, they provide an excellent calibration for these.

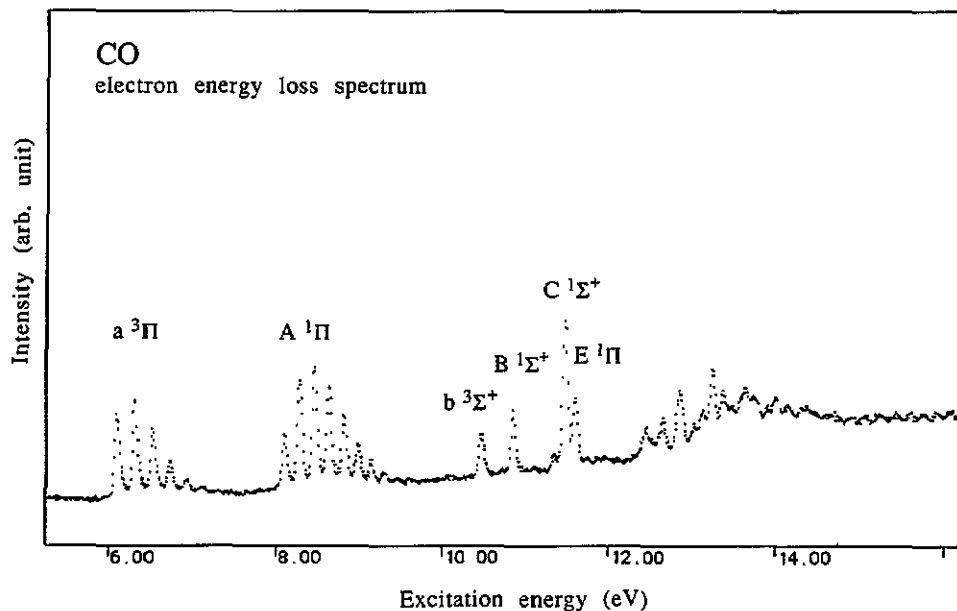


Figure 6. An electron impact spectrum of the CO molecule showing the line structure of interest for the interpretation of electron scattering contributions in the photoelectron spectrum.

As a consequence of this result, the interpretation of certain lines in the absorption spectrum in terms of Rydberg series leading to the sixth PES progression proposed by Åsbrink *et al* should be reconsidered. This also influences the potential energy diagram calculated by Locht (1977) and based on the earlier PES data.

#### 4.4. The 27–30 eV range

This region is included in figures 1, 2 and 5. The first part contains a rounded structureless band between about 27 and 27.7 eV with three superimposed narrow lines that are similar in both spectra of figure 5. The narrow lines are absent in the spectra taken with synchrotron radiation (figure 2) and monochromatized He II radiation (Carlsson Göthe 1990). They therefore correspond to states excited by He II $\beta$  radiation, while the rounded band can be associated with transitions to the  $3^2\Pi$  state, as shown by the calculations. This state, which has a leading  $4\sigma^{-1}5\sigma^{-1}2\pi^1$  configuration, is found to be repulsive (cf below).

As can be seen from figure 5 and by comparison with the spectrum taken with monochromatized He II $\alpha$  radiation, the main part of the complex line structure above 27.7 eV does not reflect states in this region but is partly due to inelastic scattering of photoelectrons from the  $4\sigma$  orbital, and partly due to states of higher energy excited by the He II $\beta$  component. In this case, the scattering involves excitation to the A  $1\Pi$  state of CO. Although some intensity remains even in the low pressure spectrum, there is no clear indication of lines that can be associated with an electronic state in this region. This is in agreement with the present calculations which did not locate any bound state of the proper symmetry in this range.

## 4.5. The 30–46 eV range

An inspection of figure 2 shows that photoelectron bands are present at about 32, 33, 34, 35, 36.5, 38, 39 and 45 eV. This essentially agrees with the xps study by Svensson *et al* using Al K $\alpha$  radiation at 1487 eV, although the relative intensities are different. In the highly resolved synchrotron radiation excited spectrum extensive fine structure is seen, probably associated with vibrational states. To show this more clearly, the

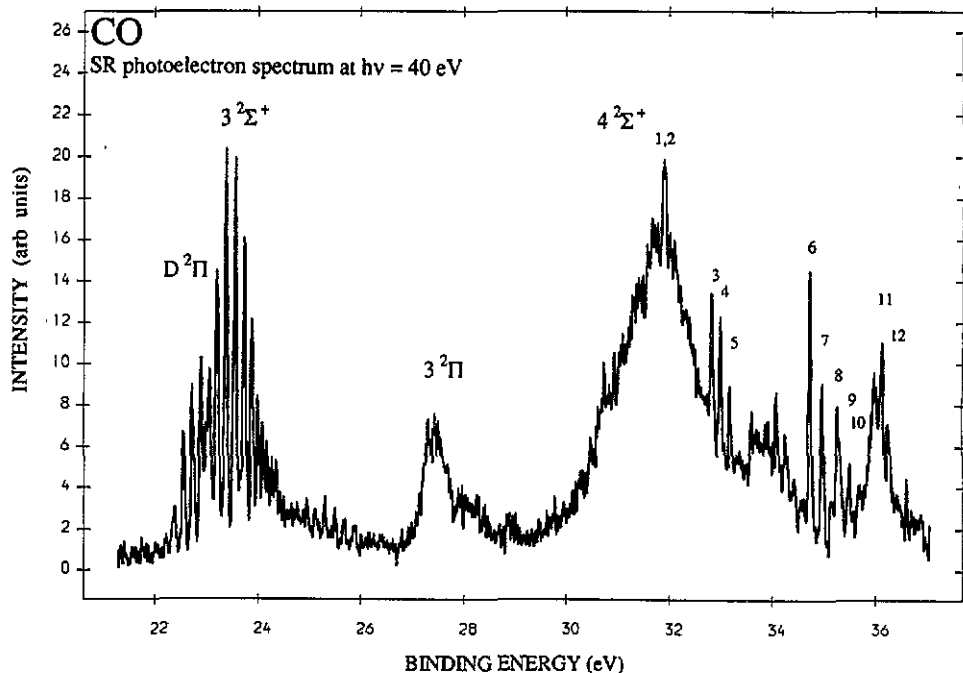


Figure 7. The synchrotron radiation excited photoelectron spectrum of CO between 22 eV and 37 eV obtained at a photon energy of 40 eV.

spectrum excited with synchrotron radiation at 40 eV is shown in figure 7. Narrow lines are present at the same positions in both spectra as well as in spectra obtained at 36 eV and 44 eV. These lines are numbered from 1 to 17. The energies and  $\beta$  values are collected in table 4. Most of these lines can be identified with lines reported by Liu *et al*, but the energies there are generally 30–70 meV higher than ours.

Line 1 is strong in all spectra whereas line 2 has a high intensity only in the spectrum recorded at 36 eV photon energy. These two lines also have different  $\beta$  values (cf table 4) which could suggest that they are associated with different electronic states. On the other hand, the spacing of 0.18 eV could correspond to a vibrational excitation. Since the lines are comparatively broad the state could be distorted by interaction with a repulsive state.

Lines 3, 4 and 5 can be identified with structures observed using He II $\beta$  excitation (figure 5). The spacings and relative intensities suggest that they form a perturbed vibrational progression as indicated by a gradually increasing spacing and a loss of intensity after the third line. The lines are more or less double, with splittings that cannot be observed in the SR spectra. These splittings may be due to spin-orbit interaction. The lines have different  $\beta$  values and their intensities also depend on photon energy, possibly

**Table 4.** Binding energies and  $\beta$  values in the 30 to 45 eV energy range obtained from photoelectron spectra excited with synchrotron radiation. Energy separations are given between lines that may belong to vibrational progressions. Energies given with three decimals are obtained from the He  $\pi\beta$  spectra. Errors shown represent one standard deviation from the mean value.

Line no	Binding energy (eV)	Energy separation (meV)	$\beta$ value			
			36 eV ( $\pm 0.2$ )	40 eV ( $\pm 0.3$ )	44 eV ( $\pm 0.4$ )	46.4 eV ( $\pm 0.4$ )
1	31.9		0.68	2	1.77	0.78
2	32.08		1.18			
3	32.826, 32.853		0.90	1.04	1.64	1.29
4	32.988, 33.045	162	0.40	0.65		
5	33.176, 33.226	188	0.93	0.39		
6	34.722			1.12	0.89	0.93
7	34.962	240		0.59	0.65	0.91
8	35.254	292			1.42	0.11
9	35.476	222			1.41	0.15
10	35.79	314				2.0
11	36.113, 36.159	159		0.88	0.47	1.77
12	36.268, 36.321	122		1.34		0.26
13	37.58					0.48
14	37.98					
15	38.68					0.38
16	38.98					
17	44.48					

due to state mixing. These three lines are followed by a band of lower intensity around 34 eV. It may contain a weak fine structure with spacings of about 170 meV, but since we were unable to identify a corresponding progression in the spectrum due to He  $\pi\beta$  radiation (cf above), this is uncertain.

Lines 6–10 are very well resolved and seem to form a vibrational progression (cf figures 2 and 7). They also correspond to well defined structures in the He  $\pi\beta$  excited spectrum in the 27–28 eV range (figure 5). The energies are therefore determined accurately (table 4). The spacings are somewhat irregular so if the lines reflect a vibrational progression the levels are strongly perturbed. Also the following photoelectron band beginning at about 36 eV appears to contain a short vibrational progression, lines 11 and 12. It may have a counterpart in the He  $\pi\beta$  excited spectrum, but these structures, like those corresponding to lines 3, 4 and 5, seem to be double.

The next photoelectron band observed between 38 and 40 eV is commonly associated with electronic states of  ${}^2\Sigma^+$  symmetry that have a leading  $3\sigma^{-1}$  configuration (Ågren and Arneberg 1983). The band is seen in figure 2 and displays superimposed fine structure. This can be interpreted in terms of one short progression starting with line 13 and another with line 15.

Finally, close to threshold at about 46 eV another band is formed. It seems to have no counterpart in the x-ray photoelectron spectrum and is probably an artefact resulting from the procedure used to subtract the background in the SR spectrum. A similar structure is seen at 42.5 eV in the spectrum excited with 44 eV photons and, as can be seen from figure 2, there is no band at this energy. However, in figure 2 a narrow line can be observed which we tentatively associate with a state of  $CO^+$  and refer to as line 17.

## 5. Discussion

Potential curves have been calculated for states of  ${}^2\Sigma^+$  and of  ${}^2\Pi$  symmetry, which are important for interpretation of the photoelectron spectrum. From these curves, vibrational energies and Franck–Condon factors were calculated for the D  ${}^2\Pi$  and  $3^2\Sigma^+$  states and the results are collected in tables 1 and 2. The theoretical vibrational energy levels and wavefunctions were obtained by solving the Schrödinger equation numerically (Le Roy 1984).

A minimum in the potential curve was obtained for the four lowest states of  ${}^2\Sigma^+$  symmetry. These curves are shown in figure 8. At still higher energies it was not possible to obtain bound states, but all curves were found to be repulsive including the states with a dominating  $3\sigma^{-1}$  configuration. The energies are in good agreement with the experimental results. As can be seen from table 2, the vibrational energies for the  $3^2\Sigma^+$  state differ by at most 25 meV from the experimental data. The highest observed level is  $v=12$  at 24.489 eV, which is 0.162 eV above the dissociation limit at 24.327 eV calculated by Huber and Herzberg (1979) from the CO dissociation energy and atomic data from Moore (1949). Thus, the experimental data support the earlier conclusion by Carlsson Göthe *et al* that there is a small barrier in the potential curve at a large internuclear distance. This is also supported by our calculations, which show a maximum in the potential curve at 2.0 Å.

For the  $4^2\Sigma^+$  state a shallow minimum is predicted in the potential curve at a very large internuclear distance, where the Franck–Condon region crosses the potential curve in a repulsive part. Transitions to this state are thus expected to give rise to a structureless photoelectron band centred at 30 eV. This most likely corresponds to a large part of the very broad band centred at 32 eV. In the high energy part of this band there may be contributions also from the  $5^2\Sigma^+$  state predicted in this energy range by Ågren and Arneberg (1983). The sharp peak containing the lines 1 and 2 most probably has a different origin.

Only two states of  ${}^2\Pi$  symmetry were found to be stable, the outer valence A  ${}^2\Pi$  state and the inner valence D  ${}^2\Pi$  state. The next stage,  $3^2\Pi$ , is repulsive everywhere as can be seen from figure 9 which displays the potential curves. From these curves, the

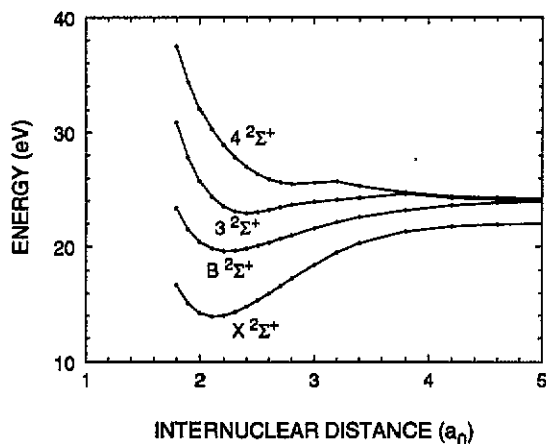


Figure 8. Calculated potential curves for  ${}^2\Sigma^+$  states. The energy scale is referred to the zero level of the neutral ground state.

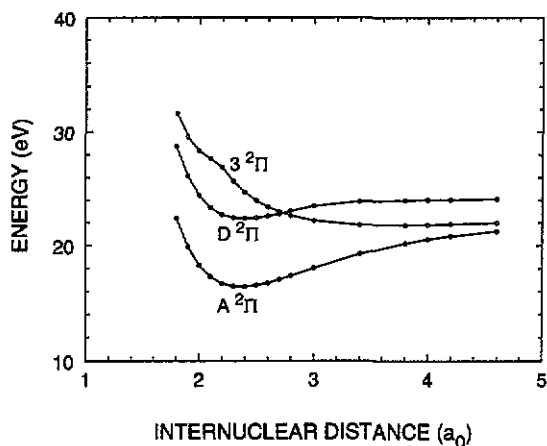


Figure 9. Calculated potential curves for  ${}^2\Pi$  states. The energy scale is referred to the zero level of the neutral ground state.

vibrational energies and relative intensities, obtained using a constant electronic transition moment equal to unity, were calculated (Le Roy 1984). The data for the  $\text{D } {}^2\Pi$  state are presented in table 1. The vibrational structures of both the  $\text{A } {}^2\Pi$  state seen by Edvardsson *et al* (1994) and the  $\text{D } {}^2\Pi$  state are very well predicted which gives another strong indication that the line at 22.376 eV, rather than the other alternatives at lower energy in the experimental spectrum, corresponds to the 0-0 transition of the  $\text{D } {}^2\Pi$  state (cf table 1).

The centre of the Franck-Condon region crosses the  $3{}^2\Pi$  state at about 27.4 eV, i.e. close to the centre of the rounded photoelectron band observed at this energy. Furthermore, a calculation of the Franck-Condon density using a program from Le Roy (1989) at some different energies is in qualitative agreement with the experimental spectrum. These results are summarized in table 5.

At 22.9 eV a curve crossing is predicted between the  $\text{D } {}^2\Pi$  and  $3{}^2\Pi$  states (figure 9). In this energy range an interaction between the states takes place which influences the vibrational structure. If the non-crossing rule is adopted, the vibrational structure would be expected to disappear above the crossing point. This is obviously not true, but the vibrational structure calculated for the  $\text{D } {}^2\Pi$  state without consideration of interaction with the  $3{}^2\Pi$  state reproduces essentially the experimental result (cf table 1). As was mentioned above, close to the predicted position of the curve crossing, the

Table 5. Franck-Condon densities for ionization from  $\text{CO } {}^1\Sigma^+$  to the repulsive  $3{}^2\Pi$  state.

Electron binding energy (eV)	Franck-Condon density
24.927	0.43
25.547	3.35
26.167	13.4
26.787	40.6
27.407	100
28.026	37.8
28.274	7.0

vibrational lines are broadened and the spacings are somewhat irregular, which may suggest that a strong local interaction limits the lifetime of the states. Assuming that the lifetime broadenings add quadratically to the other contributions to the linewidth and that these correspond to the width of the narrowest lines, i.e. 25.9 meV (cf table 1) a lifetime broadening of 26.0 meV is obtained for the  $v=4$  level. This corresponds to a lifetime of about  $2.5 \times 10^{-14}$  s. For lower and higher levels no broadening can be observed that appears to be related to the presence of the curve crossing (the larger width obtained for  $v=7$  and 9 is probably caused by the overlapping lines). This parallels the behaviour observed by Baltzer *et al* (1992b) for the  $3^2\Pi_u$  state of  $O_2^+$ , where a curve crossing occurs leading to a local interaction rather than a strongly avoided crossing.

The interaction between the  $D^2\Pi$  and  $3^2\Pi$  states is expected to lead to dissociation of the ion. A steep onset in the production of  $C^+$  ions has been observed at 555 Å (22.34 eV) and it was found by Erman *et al* (1994) that the intensity persists over the entire range of the  $D^2\Pi$  state. It was concluded that the predissociation was caused by a repulsive  $CO^+$  state dissociating into  $C^+$  ( $^2P^o$ ) +  $O(^3P)$ . Although the present results indicate that the strongest interaction should occur at  $v=4$ , the interaction with the  $3^2\Pi$  state may well lead to predissociation even below the crossing point, and this can be observed on the time scale of the mass spectroscopic experiment.

Since the potential curves associated with valence states are repulsive above the  $4^2\Sigma^+$  state, the extensive vibrational structure observed above 30 eV must be of a different origin. Most likely, it is due to Rydberg states formed in the cation. These states are expected to resemble the doubly ionized states observed in the Auger electron spectrum and could exhibit somewhat similar vibrational excitations. However, the bond distance is very sensitive to the electron configuration, so the relative intensities may differ considerably from those observed in the Auger spectrum by Correia *et al* (1985). The first part of the Auger spectrum shows rich vibrational structure with progressions where the spacings are around 180–200 meV. A likely interpretation of the photoelectron spectrum is that Rydberg series containing similar progressions are superimposed upon the broad structureless features representing transitions to valence states.

The vibrational structure in the Auger electron spectrum is resolved in the three outermost bands appearing at 41.70 eV,  $\approx 42.5$  eV and 45.40 eV. They correspond to the  $X^1\Sigma^+$ ,  $A^1\Pi$  and  $B^1\Sigma^+$  states of the  $CO^{2+}$  dication. Assuming that the photoelectron spectrum contains Rydberg series converging to these energies, most of the structure can be readily explained by ionization from the  $5\sigma$ ,  $1\pi$  and  $4\sigma$  orbitals accompanied by a  $5\sigma \rightarrow nl$  excitation, where  $n \geq 3$ . Using a quantum defect of about 0.65, which seems reasonable, one finds that the first vibrational component corresponds well with lines 1, 11 and 15 for the first series with  $n=3, 4$  and 5, respectively. Lines 3 and 13 represent the second series with  $n=3$  and 4 and lines 6 and 15 fit with the third series with  $n=3$  and 4. Lines 3 and 11 have clear counterparts in the He  $\Pi\beta$  excited spectrum where they appear to be split by about 50 meV. This could be due to spin-orbit interaction which would suggest that these states have  $\Pi$  symmetry. This interpretation, although it gives reasonable agreement with the observed lines, is not unique and in order to obtain a safe assignment additional theoretical studies are needed, with methods particularly suited for calculations of Rydberg states and transitions.

## 6. Conclusions

The study shows that the inner valence photoelectron spectrum of the CO molecule is best analysed in terms of two parts with rather different character; one with a few well

defined photoelectron bands between 20 and 30 eV and another above 30 eV with numerous narrow lines superimposed on heavily overlapping broad bands.

In the region between 20 and 30 eV three photoelectron bands have been identified corresponding to transitions to the  $\text{D}^2\Pi$ ,  $3^2\Sigma^+$  and  $3^2\Pi$  states with intensity maxima at about 22.9 eV, 23.5 eV and 27.4 eV, respectively. The progressions observed in the 24.6–27 eV and 27.6–29 eV ranges in previous studies have been shown to be caused by inelastic scattering processes and excitations with He  $\text{II}\beta$  radiation. New potential curves covering the 20–30 eV region have been calculated. A remarkable broadening is observed of the  $v=3$  and 4 vibrational lines of the  $\text{D}^2\Pi$  state. It is associated with a strong interaction with the repulsive  $3^2\Pi$  state in this region leading to predissociation via a curve crossing.

In the innermost region above 30 eV the broad bands are explained in terms of  $\text{C1}$  satellites related to both the inner valence  $3\sigma^{-1}$  single hole state and to outer valence two-hole-one-particle configurations. The superimposed narrow lines, which correspond to a very low total photoelectron intensity, are associated with vibrational states of Rydberg series converging towards the three outermost states of the dication, which contain extensive vibrational structure.

### Acknowledgment

This work was supported by the Swedish Natural Science Research Council (NFR), by the US Department of Energy, Office of Energy Research, Office of Environmental Research, under contract no W-31-109-ENG-38, and by the Science and Engineering Research Council, UK.

### References

- Ågren H and Arneberg R 1983 *Phys. Scr.* **28** 890  
Åsbrink L, Fridh C, Lindholm L and Codling K 1974 *Phys. Scr.* **10** 183  
Bagus P S and Viinikka E K 1977 *Phys. Rev. A* **15** 1486  
Baltzer P 1994 to be published  
Baltzer P and Karlsson L 1989 *Uppsala University Institute of Physics Report* UUIP-1211  
Baltzer P, Karlsson L, Lundqvist M and Wannberg B 1993 *Rev. Sci. Instrum.* **64** 2179  
Baltzer P, Larsson M, Karlsson L, Wannberg B and Carlsson Göthe M 1992a *Phys. Rev. A* **46** 5545  
Baltzer P, Wannberg B, Karlsson L, Carlsson Göthe M and Larsson M 1992b *Phys. Rev. A* **45** 4374  
Banna M S and Shirley D A 1976 *J. Electron Spectrosc.* **8** 255  
Carlsson Göthe M 1990 *Acta Universitatis Upsaliensis* **292** (thesis)  
Carlsson Göthe M, Wannberg B, Falk F, Karlsson L, Svensson S and Baltzer P 1991 *Phys. Rev. A* **44** R17  
Cederbaum L S and Domcke W 1977 *Adv. Chem. Phys.* **36** 205  
Cederbaum L S, Domcke W, Schirmer J and von Niessen W 1980 *Phys. Scr.* **21** 481  
Codling K and Potts A W 1974 *J. Phys. B: At. Mol. Phys.* **7** 163  
Correia N, Flores-Riveros A, Ågren H, Helenelund K, Asplund L and Gelius U 1985 *J. Chem. Phys.* **83** 2035  
Eberhardt W, Plummer E W, Lyo I-W, Murphy R, Carr R and Ford W K J 1987 *J. Physique Coll.* **C9** (suppl. 12) 697  
Edvardsson D, Baltzer P, Lundqvist M, Wannberg B and Karlsson L 1994 to be published  
Erman P, Rachlew-Källine E and Sorensen S L 1994 *Z. Phys. D* **30** 315  
Gelius U, Basilier E, Svensson S, Bergmark T and Siegbahn, K 1973 *J. Electron Spectrosc.* **3** 405  
Honjou N and Yarkony D R 1985 *J. Phys. Chem.* **89** 44  
Huber K P and Herzberg G 1979 *Molecular Spectra and Molecular Structure IV. Constants of Diatomic Molecules* (New York: Van Nostrand Reinhold)  
Krummacher S, Schmidt V and Wulleumier F 1980 *J. Phys. B: At. Mol. Phys.* **13** 3993

- Krummacher S, Schmidt V, Wuilleumier F, Bizeau J M and Ederer D L 1983, *J. Phys. B: At. Mol. Phys.* **16** 1733
- Langhoff P W, Langhoff S R, Rescigno T N, Schirmer J, Cederbaum L S and Domcke W 1981 *Chem. Phys.* **58** 71
- Lavendy H, Robbe J M and Flament J P 1993, *Chem. Phys. Lett.* **205** 456
- Le Roy R J 1984 *Chem. Phys. Res. Report* CP-230R (University of Waterloo, Ontario, Canada)
- 1989 *Comput. Phys. Commun.* **52** 383
- Lie G C and Clementi E 1974 *J. Chem. Phys.* **60** 1275
- Liu Z F, Bancroft G M, Coatsworth L H and Tan K H 1993 *Chem. Phys. Lett.* **203** 337
- Locht R 1977 *Chem. Phys.* **22** 13
- Martin R L and Shirley D A 1976 *Phys. Rev. A* **13** 1475
- Moore C E 1949 *Atomic Transition Probabilities* (NBS circular no 467) (Washington, DC: US Govt Printing Office)
- Nyholm R, Berndtsson A, Nilsson R, Hedman J and Nordling C 1977 *Phys. Scr.* **16** 383
- Okuda M and Jonathan N 1974 *J. Electron Spectrosc.* **3** 19
- Parr A C, Southworth S H, Dehmer J L and Holland D M P 1984 *Nucl. Instrum. Methods* **222** 221
- Potts A W and Williams T A 1974 *J. Electron Spectrosc.* **3** 3
- Schirmer J, Cederbaum L S, Domcke W and von Niessen W 1977 *Chem. Phys.* **26** 149
- Schlag E W, Peatman W B and Müller-Dethlefs K 1993 *J. Electron Spectrosc.* **66** 139
- Siegbahn P E M 1983 *Int. J. Quantum Chem.* **23** 1869
- Siegbahn P E M, Almlöf J, Heiberg A and Roos B O 1981 *J. Chem. Phys.* **74** 2384
- Svensson S, Carlsson Göthe M, Karlsson L, Nilsson A, Mårtensson N and Gelius U 1991 *Phys. Scr.* **44** 184
- Turner D W, Baker C, Baker A D and Brundle C R 1970 *Molecular Photoelectron Spectroscopy* (London: Wiley-Interscience)
- van Duijneveldt F B 1971 *IBM Res. Rep.* **945** (December)
- Wannberg B, Nordfors D, Tan K L, Karlsson L and Mattsson L 1988 *J. Electron Spectrosc.* **47** 147